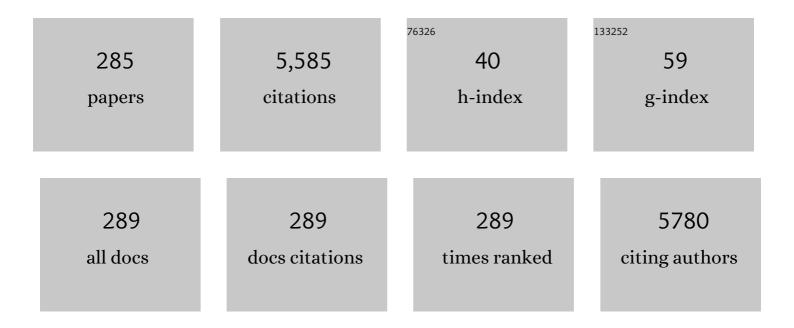
## Patrick Wagner

List of Publications by Year in descending order

Source: https://exaly.com/author-pdf/4324458/publications.pdf Version: 2024-02-01



#	Article	IF	CITATIONS
1	Low Cost, Sensitive Impedance Detection of <i>E. coli</i> Bacteria in Foodâ€Matrix Samples Using Surfaceâ€Imprinted Polymers as Wholeâ€Cell Receptors. Physica Status Solidi (A) Applications and Materials Science, 2022, 219, 2100405.	1.8	5
2	Integrating Thermal Sensors in a Microplate Format: Simultaneous Real-Time Quantification of Cell Number and Metabolic Activity. ACS Applied Materials & Interfaces, 2022, 14, 2440-2451.	8.0	3
3	Ionic strength tunes yeast viscoelasticity and promotes trace-level cell detection. Physics in Medicine, 2022, 14, 100049.	1.3	3
4	Field-Effect Capacitors Decorated with Ligand-Stabilized Gold Nanoparticles: Modeling and Experiments. Biosensors, 2022, 12, 334.	4.7	2
5	Depletion of wild-type target enhances the hybridization-based sensitivity of low-abundant mutation detection by reference capture probes. Sensors and Actuators B: Chemical, 2022, 368, 132175.	7.8	2
6	Synchronized, Spontaneous, and Oscillatory Detachment of Eukaryotic Cells: A New Tool for Cell Characterization and Identification. Advanced Science, 2022, 9, .	11.2	4
7	Electropolymerized Receptor Coatings for the Quantitative Detection of Histamine with a Catheter-Based, Diagnostic Sensor. ACS Sensors, 2021, 6, 100-110.	7.8	7
8	Ionic strength controls long-term cell-surface interactions – A QCM-D study of S. cerevisiae adhesion, retention and detachment. Journal of Colloid and Interface Science, 2021, 585, 583-595.	9.4	12
9	Introducing a Thermal-Based Method for Measuring Dynamic Thin Film Thickness in Real Time as a Tool for Sensing Applications. IEEE Transactions on Instrumentation and Measurement, 2021, 70, 1-10.	4.7	5
10	Measuring Thermal Conductivity in a Microfluidic Device With the Transient Thermal Offset (TTO) Method. IEEE Sensors Journal, 2021, 21, 7298-7307.	4.7	4
11	Pulsed Thermal Method for Monitoring Cell Proliferation in Real-Time. Sensors, 2021, 21, 2440.	3.8	5
12	Selective Campylobacter detection and quantification in poultry: A sensor tool for detecting the cause of a common zoonosis at its source. Sensors and Actuators B: Chemical, 2021, 332, 129484.	7.8	17
13	The hot-wire concept: Towards a one-element thermal biosensor platform. Biosensors and Bioelectronics, 2021, 179, 113043.	10.1	7
14	Light-Addressable Actuator-Sensor Platform for Monitoring and Manipulation of pH Gradients in Microfluidics: A Case Study with the Enzyme Penicillinase. Biosensors, 2021, 11, 171.	4.7	18
15	Detection of yeast strains by combining surface-imprinted polymers with impedance-based readout. Sensors and Actuators B: Chemical, 2021, 340, 129917.	7.8	13
16	Assessing the impact of exposome on the course of chronic obstructive pulmonary disease and cystc fibrosis. Environmental Epidemiology, 2021, 5, e165.	3.0	4
17	Formation of controllable pH gradients inside microchannels by using light-addressable electrodes. Sensors and Actuators B: Chemical, 2021, 346, 130422.	7.8	4
18	Passive permeability assay of doxorubicin through model cell membranes under cancerous and normal membrane potential conditions. European Journal of Pharmaceutics and Biopharmaceutics, 2020, 146, 133-142.	4.3	11

#	Article	IF	CITATIONS
19	Searching for a common origin of heat-transfer effects in bio- and chemosensors: A study on thiols as a model system. Sensors and Actuators B: Chemical, 2020, 310, 127627.	7.8	6
20	Development of a package-sterilization process for aseptic filling machines: A numerical approach and validation for surface treatment with hydrogen peroxide. Sensors and Actuators A: Physical, 2020, 303, 111691.	4.1	9
21	An imaging study and spectroscopic curing analysis on polymers for synthetic whole-cell receptors for bacterial detection. Japanese Journal of Applied Physics, 2020, 59, SD0802.	1.5	2
22	LAPS-based monitoring of metabolic responses of bacterial cultures in a paper fermentation broth. Sensors and Actuators B: Chemical, 2020, 320, 128232.	7.8	9
23	QCM-D Study of Time-Resolved Cell Adhesion and Detachment: Effect of Surface Free Energy on Eukaryotes and Prokaryotes. ACS Applied Materials & Interfaces, 2020, 12, 18258-18272.	8.0	43
24	Understanding the Dehydration Stress in Lipid Vesicles by a Combined Quartz Crystal Microbalance and Dielectric Spectroscopy Study. Physica Status Solidi (A) Applications and Materials Science, 2020, 217, 1900986.	1.8	4
25	Towards a catheter-based impedimetric sensor for the assessment of intestinal histamine levels in IBS patients. Biosensors and Bioelectronics, 2020, 158, 112152.	10.1	13
26	Measuring Thermal Conductivity in a Microfluidic Device with the Transient Thermal Offset (TTO) Method. , 2020, , .		0
27	A LAPS-Based Differential Sensor for Parallelized Metabolism Monitoring of Various Bacteria. Sensors, 2019, 19, 4692.	3.8	11
28	Development of an in-line evaporation unit for the production of gas mixtures containing hydrogen peroxide – numerical modeling and experimental results. International Journal of Heat and Mass Transfer, 2019, 143, 118519.	4.8	4
29	Quantitative differential monitoring of the metabolic activity of Corynebacterium glutamicum cultures utilizing a light-addressable potentiometric sensor system. Biosensors and Bioelectronics, 2019, 139, 111332.	10.1	11
30	Sensitive and specific detection of E. coli using biomimetic receptors in combination with a modified heat-transfer method. Biosensors and Bioelectronics, 2019, 136, 97-105.	10.1	43
31	Laser-Grafted Molecularly Imprinted Polymers for the Detection of Histamine from Organocatalyzed Atom Transfer Radical Polymerization. Macromolecules, 2019, 52, 2304-2313.	4.8	27
32	A compact device for simultaneous dielectric spectroscopy and microgravimetric analysis under controlled humidity. Review of Scientific Instruments, 2019, 90, 125106.	1.3	1
33	Cell detection by surface imprinted polymers SIPs: A study to unravel the recognition mechanisms. Sensors and Actuators B: Chemical, 2018, 255, 907-917.	7.8	41
34	Scalable fabrication and application of nanoscale IDE-arrays as multi-electrode platform for label-free biosensing. Sensors and Actuators B: Chemical, 2018, 265, 115-125.	7.8	14
35	Impedimetric Sensing of DNA with Silicon Nanowire Transistors as Alternative Transducer Principle. Physica Status Solidi (A) Applications and Materials Science, 2018, 215, 1700740.	1.8	14
36	Graphite oxide electrical sensors are able to distinguish single nucleotide polymorphisms in physiological buffers. FlatChem, 2018, 7, 1-9.	5.6	5

#	Article	IF	CITATIONS
37	SIPâ€Based Thermal Detection Platform for the Direct Detection of Bacteria Obtained from a Contaminated Surface. Physica Status Solidi (A) Applications and Materials Science, 2018, 215, 1700777.	1.8	3
38	ScFv-modified graphene-coated IDE-arrays for â€~label-free' screening of cardiovascular disease biomarkers in physiological saline. Biosensors and Bioelectronics, 2018, 102, 574-581.	10.1	20
39	A Novel Modular Device for Biological Impedance Measurements: The Differential Impedimetric Sensor Cell (DISC). Physica Status Solidi (A) Applications and Materials Science, 2018, 215, 1701029.	1.8	3
40	Thermocatalytic Behavior of Manganese (IV) Oxide as Nanoporous Material on the Dissociation of a Gas Mixture Containing Hydrogen Peroxide. Nanomaterials, 2018, 8, 262.	4.1	29
41	Cell detection by surface imprinted polymers (SIPs) — A study of the sensor surface by optical and dielectric relaxation spectroscopy. IEEE Transactions on Dielectrics and Electrical Insulation, 2018, 25, 816-821.	2.9	7
42	Experimental and Numerical Analyzes of a Sensor Based on Interdigitated Electrodes for Studying Microbiological Alterations. Physica Status Solidi (A) Applications and Materials Science, 2018, 215, 1700920.	1.8	1
43	Optimization of Cellâ€Based Multiâ€Chamber LAPS Measurements Utilizing FPGAâ€Controlled Laserâ€Diode Modules. Physica Status Solidi (A) Applications and Materials Science, 2018, 215, 1800058.	1.8	6
44	Electrochemical Evaluation of Lightâ€Addressable Electrodes Based on TiO <sub>2</sub> for the Integration in Labâ€on hip Systems. Physica Status Solidi (A) Applications and Materials Science, 2018, 215, 1800150.	1.8	5
45	High Electronic Conductance through Double-Helix DNA Molecules with Fullerene Anchoring Groups. Journal of Physical Chemistry A, 2017, 121, 1182-1188.	2.5	30
46	Optimization and characterization of a flow cell for heat-transfer-based biosensing. Physica Status Solidi (A) Applications and Materials Science, 2017, 214, 1600758.	1.8	8
47	Development of an impedimetric sensor for the label-free detection of the amino acid sarcosine with molecularly imprinted polymer receptors. Sensors and Actuators B: Chemical, 2017, 246, 461-470.	7.8	65
48	Biomimetic Bacterial Identification Platform Based on Thermal Wave Transport Analysis (TWTA) through Surface-Imprinted Polymers. ACS Infectious Diseases, 2017, 3, 388-397.	3.8	33
49	Label-Free Detection of Small Organic Molecules by Molecularly Imprinted Polymer Functionalized Thermocouples: Toward In Vivo Applications. ACS Sensors, 2017, 2, 583-589.	7.8	31
50	Differential imaging of the metabolism of bacteria and eukaryotic cells based on light-addressable potentiometric sensors. Electrochimica Acta, 2017, 246, 234-241.	5.2	24
51	Anisotropic InÂSitu-Coated AuNPs on Screen-Printed Carbon Surface for Enhanced Prostate-Specific Antigen Impedimetric Aptasensor. Journal of Electronic Materials, 2017, 46, 3542-3552.	2.2	16
52	Engineering of Functional Interfaces. Physica Status Solidi (A) Applications and Materials Science, 2017, 214, 1770154.	1.8	0
53	From colossal magnetoresistance to solar cells: An overview on 66 years of research into perovskites. Physica Status Solidi (A) Applications and Materials Science, 2017, 214, 1700394.	1.8	15
54	Real-time monitoring of interactions between Ebola fusion peptide and solid-supported phospholipid membranes: Effect of peptide concentration and layer geometry. Physics in Medicine, 2017, 4, 1-7.	1.3	9

#	Article	IF	CITATIONS
55	Heat Transfer as a New Sensing Technique for the Label-Free Detection of Biomolecules. Springer Series on Chemical Sensors and Biosensors, 2017, , 383-407.	0.5	1
56	Single-Shot Detection of Neurotransmitters in Whole-Blood Samples by Means of the Heat-Transfer Method in Combination with Synthetic Receptors. Sensors, 2017, 17, 2701.	3.8	16
57	On-Line Monitoring of the Metabolic Activity of Bacteria and Eukaryotic Cells Utilizing Light-Addressable Potentiometric Sensors. Proceedings (mdpi), 2017, 1, 716.	0.2	1
58	FEM-based modeling of a calorimetric gas sensor for hydrogen peroxide monitoring. Physica Status Solidi (A) Applications and Materials Science, 2017, 214, 1600912.	1.8	6
59	Formation and electrical characterization of black lipid membranes in porous filter materials. Physica Status Solidi (A) Applications and Materials Science, 2017, 214, 1700104.	1.8	4
60	Determination of the extracellular acidification of <i>Escherichia coli</i> K12 with a multiâ€chamberâ€based LAPS system. Physica Status Solidi (A) Applications and Materials Science, 2016, 213, 1479-1485.	1.8	20
61	DNA detection with top–down fabricated silicon nanowire transistor arrays in linear operation regime. Physica Status Solidi (A) Applications and Materials Science, 2016, 213, 1510-1519.	1.8	13
62	Fabrication of optomicrofluidics for real-time bioassays based on hollow sphere colloidal photonic crystals with wettability patterns. Journal of Materials Chemistry C, 2016, 4, 7853-7858.	5.5	27
63	Label-Free Detection of <i>Escherichia coli</i> Based on Thermal Transport through Surface Imprinted Polymers. ACS Sensors, 2016, 1, 1140-1147.	7.8	64
64	A Review on Synthetic Receptors for Bioparticle Detection Created by Surface-Imprinting Techniques—From Principles to Applications. ACS Sensors, 2016, 1, 1171-1187.	7.8	99
65	Engineering of Functional Interfaces 2016. Physica Status Solidi (A) Applications and Materials Science, 2016, 213, 1393-1394.	1.8	0
66	Improved Molecular Imprinting Based on Colloidal Particles Made from Miniemulsion: A Case Study on Testosterone and Its Structural Analogues. Macromolecules, 2016, 49, 2559-2567.	4.8	23
67	Heat-transfer based characterization of DNA on synthetic sapphire chips. Sensors and Actuators B: Chemical, 2016, 230, 260-271.	7.8	10
68	Light-addressable Potentiometric Sensor (LAPS) Combined with Multi-chamber Structures to Investigate the Metabolic Activity of Cells. Procedia Engineering, 2015, 120, 384-387.	1.2	9
69	Engineering of Functional Interfaces. Physica Status Solidi (A) Applications and Materials Science, 2015, 212, 1183-1183.	1.8	0
70	Graphite oxide multilayers for device fabrication: Enzymeâ€based electrical sensing of glucose. Physica Status Solidi (A) Applications and Materials Science, 2015, 212, 1335-1341.	1.8	7
71	Impedimetric immunosensor for the detection of histamine based on reduced graphene oxide. Physica Status Solidi (A) Applications and Materials Science, 2015, 212, 1327-1334.	1.8	21
72	Study of Interdigitated Electrode Arrays Using Experiments and Finite Element Models for the Evaluation of Sterilization Processes. Sensors, 2015, 15, 26115-26127.	3.8	33

#	Article	IF	CITATIONS
73	Real-time analysis of dual-display phage immobilization and autoantibody screening using quartz crystal microbalance with dissipation monitoring. International Journal of Nanomedicine, 2015, 10, 5237.	6.7	2
74	Phase Transitions of Binary Lipid Mixtures: A Combined Study by Adiabatic Scanning Calorimetry and Quartz Crystal Microbalance with Dissipation Monitoring. Advances in Condensed Matter Physics, 2015, 2015, 1-14.	1.1	27
75	Monitoring of the Enzymatically Catalyzed Degradation of Biodegradable Polymers by Means of Capacitive Field-Effect Sensors. Analytical Chemistry, 2015, 87, 6607-6613.	6.5	7
76	Photonic studies on polymer-coated sapphire-spheres: A model system for biological ligands. Sensors and Actuators A: Physical, 2015, 222, 212-219.	4.1	2
77	Heat-Transfer-Method-Based Cell Culture Quality Assay through Cell Detection by Surface Imprinted Polymers. Langmuir, 2015, 31, 2043-2050.	3.5	29
78	Improving the sensitivity of the heatâ€ŧransfer method (HTM) for cancer cell detection with optimized sensor chips. Physica Status Solidi (A) Applications and Materials Science, 2015, 212, 1320-1326.	1.8	13
79	Morphological TEM studies and magnetoresistance analysis of sputtered Alâ€substituted ZnO films: The role of oxygen. Physica Status Solidi (A) Applications and Materials Science, 2015, 212, 1191-1201.	1.8	1
80	Detection of triacetone triperoxide using temperature cycled metalâ€oxide semiconductor gas sensors. Physica Status Solidi (A) Applications and Materials Science, 2015, 212, 1289-1298.	1.8	9
81	Mechanism of Nonpolar Model Substances to Inhibit Primary Gushing Induced by Hydrophobin HFBI. Journal of Agricultural and Food Chemistry, 2015, 63, 4673-4682.	5.2	2
82	Effect of Cholesterol on the Phase Behavior of Solid-Supported Lipid Vesicle Layers. Journal of Physical Chemistry B, 2015, 119, 4985-4992.	2.6	22
83	Label-free Protein Detection Based on the Heat-Transfer Method—A Case Study with the Peanut Allergen Ara h 1 and Aptamer-Based Synthetic Receptors. ACS Applied Materials & Interfaces, 2015, 7, 10316-10323.	8.0	32
84	An application of field-effect sensors for in-situ monitoring of degradation of biopolymers. Sensors and Actuators B: Chemical, 2015, 207, 954-959.	7.8	4
85	Multiple sensor-type system for monitoring the microbicidal effectiveness of aseptic sterilisation processes. Food Control, 2015, 47, 615-622.	5.5	4
86	Heat-transfer-based detection of SNPs in the PAH gene of PKU patients. International Journal of Nanomedicine, 2014, 9, 1629.	6.7	9
87	Elastic scattering from a sapphire microsphere placed on a silica optical fiber coupler: Possible applications to biosensing. European Physical Journal: Special Topics, 2014, 223, 1995-2002.	2.6	3
88	Array Formatting of the Heat-Transfer Method (HTM) for the Detection of Small Organic Molecules by Molecularly Imprinted Polymers. Sensors, 2014, 14, 11016-11030.	3.8	23
89	Enzymatically Catalyzed Degradation of Biodegradable Polymers Investigated by Means of a Semiconductor-based Field-effect Sensor. Procedia Engineering, 2014, 87, 1314-1317.	1.2	0
90	Reduced graphene oxideâ€based sensing platform for electric cell–substrate impedance sensing. Physica Status Solidi (A) Applications and Materials Science, 2014, 211, 1404-1409.	1.8	8

#	Article	lF	CITATIONS
91	Engineering of Functional Interfaces. Physica Status Solidi (A) Applications and Materials Science, 2014, 211, 1339-1339.	1.8	0
92	Melittin disruption of raft and non-raft-forming biomimetic membranes: A study by quartz crystal microbalance with dissipation monitoring. Colloids and Surfaces B: Biointerfaces, 2014, 123, 938-944.	5.0	24
93	Photonic detection and characterization of DNA using sapphire microspheres. Journal of Biomedical Optics, 2014, 19, 097006.	2.6	7
94	Capacitively coupled electrolyte-conductivity sensor based on high-k material of barium strontium titanate. Sensors and Actuators B: Chemical, 2014, 198, 102-109.	7.8	25
95	Buchwald–Hartwig reactions in water using surfactants. Tetrahedron, 2014, 70, 3413-3421.	1.9	42
96	Multiparameter Sensor Chip with Barium Strontium Titanate as Multipurpose Material. Electroanalysis, 2014, 26, 980-987.	2.9	8
97	Phase transitions in lipid vesicles detected by a complementary set of methods: heatâ€transfer measurements, adiabatic scanning calorimetry, and dissipationâ€mode quartz crystal microbalance. Physica Status Solidi (A) Applications and Materials Science, 2014, 211, 1377-1388.	1.8	41
98	Integration of heat-transfer resistance measurements onto a digital microfluidic platform towards the miniaturized and automated label-free detection of biomolecular interactions. , 2014, , .		0
99	Boronâ€Doped Diamond Functionalization by an Electrografting/Alkyne–Azide Click Chemistry Sequence. ChemElectroChem, 2014, 1, 1145-1154.	3.4	21
100	t-BuXPhos: a highly efficient ligand for Buchwald–Hartwig coupling in water. Green Chemistry, 2014, 16, 4170-4178.	9.0	62
101	Homopolymers as nanocarriers for the loading of block copolymer micelles with metal salts: a facile way to large-scale ordered arrays of transition-metal nanoparticles. Journal of Materials Chemistry C, 2014, 2, 701-707.	5.5	5
102	Heat transfer resistance as a tool to quantify hybridization efficiency of DNA on a nanocrystalline diamond surface. Diamond and Related Materials, 2014, 48, 32-36.	3.9	8
103	Rapid fabrication of micronâ€sized CVDâ€diamond structures by microfluidic contact printing. Physica Status Solidi (A) Applications and Materials Science, 2014, 211, 1448-1454.	1.8	4
104	Thermal detection of histamine with a graphene oxide based molecularly imprinted polymer platform prepared by reversible addition–fragmentation chain transfer polymerization. Sensors and Actuators B: Chemical, 2014, 203, 527-535.	7.8	59
105	The Heat-Transfer Method: A Versatile Low-Cost, Label-Free, Fast, and User-Friendly Readout Platform for Biosensor Applications. ACS Applied Materials & Interfaces, 2014, 6, 13309-13318.	8.0	59
106	Heat-Transfer Resistance Measurement Method (HTM)-Based Cell Detection at Trace Levels Using a Progressive Enrichment Approach with Highly Selective Cell-Binding Surface Imprints. Langmuir, 2014, 30, 3631-3639.	3.5	26
107	Cross-linked degradable poly(β-thioester) networks via amine-catalyzed thiol-ene click polymerization. Polymer, 2014, 55, 3525-3532.	3.8	22
108	Heat-transfer-based detection of l-nicotine, histamine, and serotonin using molecularly imprinted polymers as biomimetic receptors. Analytical and Bioanalytical Chemistry, 2013, 405, 6453-6460.	3.7	45

#	Article	IF	CITATIONS
109	Molecularly imprinted polymers as synthetic receptors for the QCM-D-based detection of l-nicotine in diluted saliva and urine samples. Analytical and Bioanalytical Chemistry, 2013, 405, 6479-6487.	3.7	33
110	Molecular imprinted polymer films on <scp>RFID</scp> tags: a first step towards disposable packaging sensors. Physica Status Solidi (A) Applications and Materials Science, 2013, 210, 938-944.	1.8	16
111	Selective Identification of Macrophages and Cancer Cells Based on Thermal Transport through Surface-Imprinted Polymer Layers. ACS Applied Materials & Interfaces, 2013, 5, 7258-7267.	8.0	69
112	Ultrafast Selfâ€Assembly Using Ultrasound: A Facile Route to the Rapid Fabrication of Wellâ€Ordered Dense Arrays of Inorganic Nanostructures. Angewandte Chemie - International Edition, 2013, 52, 9709-9713.	13.8	7
113	Impedimetric Detection of Histamine in Bowel Fluids Using Synthetic Receptors with pH-Optimized Binding Characteristics. Analytical Chemistry, 2013, 85, 1475-1483.	6.5	54
114	Combined amperometric/field-effect sensor for the detection of dissolved hydrogen. Sensors and Actuators B: Chemical, 2013, 187, 168-173.	7.8	8
115	Degradation of thin poly(lactic acid) films: Characterization by capacitance–voltage, atomic force microscopy, scanning electron microscopy and contact-angle measurements. Electrochimica Acta, 2013, 113, 779-784.	5.2	11
116	Mobile Application for Impedance-Based Biomimetic Sensor Readout. IEEE Sensors Journal, 2013, 13, 2659-2665.	4.7	27
117	Trisubstitution of pyridine through sequential and regioselective palladium cross-coupling reactions affording analogs of known GPR54 antagonists. RSC Advances, 2013, 3, 10296.	3.6	9
118	A critical comparison of cell-based sensor systems for the detection of Cr(VI) in aquatic environment. Sensors and Actuators B: Chemical, 2013, 182, 58-65.	7.8	27
119	Characterization of biodegradable polymers with capacitive field-effect sensors. Sensors and Actuators B: Chemical, 2013, 187, 2-7.	7.8	12
120	Metabolic responses of <i>Escherichia coli</i> upon glucose pulses captured by a capacitive fieldâ€effect sensor. Physica Status Solidi (A) Applications and Materials Science, 2013, 210, 926-931.	1.8	12
121	Implementing heat transfer resistivity as a key element in a nanocrystalline diamond based single nucleotide polymorphism detection array. Diamond and Related Materials, 2013, 38, 45-51.	3.9	12
122	Impedance spectroscopy: A tool for realâ€ŧime <i>in situ</i> monitoring of the degradation of biopolymers. Physica Status Solidi (A) Applications and Materials Science, 2013, 210, 905-910.	1.8	4
123	Chip-based amperometric enzyme sensor system for monitoring of bioprocesses by flow-injection analysis. Journal of Biotechnology, 2013, 163, 371-376.	3.8	51
124	Controlled synthesis of ultrathin ZnO nanowires using micellar gold nanoparticles as catalyst templates. Nanoscale, 2013, 5, 7046.	5.6	15
125	Routine fabrication of reduced graphene oxide microarray devices via all solution processing. Physica Status Solidi (A) Applications and Materials Science, 2013, 210, 968-974.	1.8	10
126	Preparation of epitaxial films of the transparent conductive oxide Al: <scp>Z</scp> n <scp>O</scp> by reactive highâ€pressure sputtering in Ar/ <scp>O</scp> <sub>2</sub> mixtures. Physica Status Solidi (A) Applications and Materials Science, 2013, 210, 1013-1018.	1.8	3

#	Article	IF	CITATIONS
127	Surface plasmon resonanceâ€based <scp>DNA</scp> microarrays: Comparison of thiol and phosphorothioate modified oligonucleotides. Physica Status Solidi (A) Applications and Materials Science, 2013, 210, 918-925.	1.8	3
128	Using a cell-based gas biosensor for investigation of adverse effects of acetone vapors in vitro. Biosensors and Bioelectronics, 2013, 40, 393-400.	10.1	6
129	Multiâ€sensor chip for the investigation of different types of metal oxides for the detection of H <sub>2</sub> <scp>O</scp> <sub>2</sub> in the ppm range. Physica Status Solidi (A) Applications and Materials Science, 2013, 210, 898-904.	1.8	11
130	Optimizing the Thermal Read-Out Technique for MIP-Based Biomimetic Sensors: Towards Nanomolar Detection Limits. Sensors, 2013, 13, 9148-9159.	3.8	26
131	Combining Electrochemical Impedance Spectroscopy and Surface Plasmon Resonance into one Simultaneous Read-Out System for the Detection of Surface Interactions. Sensors, 2013, 13, 14650-14661.	3.8	7
132	Characterisation of aseptic sterilisation processes using an electronic nose. International Journal of Nanotechnology, 2013, 10, 470.	0.2	2
133	Engineering of Functional Interfaces. Physica Status Solidi (A) Applications and Materials Science, 2013, 210, 845-845.	1.8	Ο
134	Reduced graphene oxide micropatterns as an interface for adherent cells. Physica Status Solidi (A) Applications and Materials Science, 2013, 210, 975-982.	1.8	9
135	Electronic monitoring of chemical <scp>DNA</scp> denaturation on nanocrystalline diamond electrodes with different molarities and flow rates. Physica Status Solidi (A) Applications and Materials Science, 2013, 210, 911-917.	1.8	3
136	Cell proliferation monitoring by multiplexed electrochemical impedance spectroscopy on microwell assays. Physica Status Solidi C: Current Topics in Solid State Physics, 2013, 10, 882-888.	0.8	2
137	Embedded Unit for Point-of-Care Impedance Based Biosensor Readout. , 2012, , .		Ο
138	MIP-based Sensor Platforms for Detection of Analytes in Nano- and Micromolar Range. , 2012, , 91-124.		1
139	Monitoring of irritant gas using a whole-cell-based sensor system. Sensors and Actuators B: Chemical, 2012, 175, 208-217.	7.8	12
140	Direct visualization of boron dopant distribution and coordination in individual chemical vapor deposition nanocrystalline B-doped diamond grains. Applied Physics Letters, 2012, 101, 041907.	3.3	61
141	Evidence for phase separation of ethanol-water mixtures at the hydrogen terminated nanocrystalline diamond surface. Journal of Chemical Physics, 2012, 137, 044702.	3.0	11
142	Impact of Functional Groups onto the Electronic Structure of Metal Electrodes in Molecular Junctions. Journal of Physical Chemistry C, 2012, 116, 21810-21815.	3.1	8
143	Analysis of an optical biosensor based on elastic light scattering from diamondâ€, glassâ€, and sapphire microspheres. Physica Status Solidi (A) Applications and Materials Science, 2012, 209, 1804-1810.	1.8	11
144	Grain size tuning of nanocrystalline chemical vapor deposited diamond by continuous electrical bias growth: Experimental and theoretical study. Physica Status Solidi (A) Applications and Materials Science, 2012, 209, 1675-1682.	1.8	33

#	Article	IF	CITATIONS
145	MIP-based biomimetic sensor for the electronic detection of serotonin in human blood plasma. Sensors and Actuators B: Chemical, 2012, 171-172, 602-610.	7.8	58
146	Analytical TEM study of CVD diamond growth on TiO2 sol–gel layers. Diamond and Related Materials, 2012, 23, 93-99.	3.9	15
147	Local boron environment in B-doped nanocrystalline diamond films. Nanoscale, 2012, 4, 5960.	5.6	46
148	Heat-Transfer Resistance at Solid–Liquid Interfaces: A Tool for the Detection of Single-Nucleotide Polymorphisms in DNA. ACS Nano, 2012, 6, 2712-2721.	14.6	74
149	Development of multichannel quartz crystal microbalances for MIPâ€based biosensing. Physica Status Solidi (A) Applications and Materials Science, 2012, 209, 892-899.	1.8	26
150	Microfluidic chip with integrated microvalves based on temperature―and pHâ€responsive hydrogel thin films. Physica Status Solidi (A) Applications and Materials Science, 2012, 209, 839-845.	1.8	23
151	Detection of <scp>L</scp> â€nicotine with dissipation mode quartz crystal microbalance using molecular imprinted polymers. Physica Status Solidi (A) Applications and Materials Science, 2012, 209, 905-910.	1.8	9
152	Engineering of Functional Surfaces and Interfaces. Physica Status Solidi (A) Applications and Materials Science, 2012, 209, 803-804.	1.8	0
153	Controlling aseptic sterilization processes by means of a multi-sensor system. , 2011, , .		1
154	Influence of Interface Morphology onto the Photovoltaic Properties of Nanopatterned ZnO/Poly(3-hexylthiophene) Hybrid Solar Cells. An Impedance Spectroscopy Study. Journal of Physical Chemistry C, 2011, 115, 16695-16700.	3.1	45
155	Hierarchical Carbon Nanowire Microarchitectures Made by Plasma-Assisted Pyrolysis of Photoresist. ACS Nano, 2011, 5, 6593-6600.	14.6	55
156	One-chip integrated dual amperometric/field-effect sensor for the detection of dissolved hydrogen. Procedia Engineering, 2011, 25, 1161-1164.	1.2	2
157	Air Quality Monitoring using a Whole-Cell based Sensor System. Procedia Engineering, 2011, 25, 1421-1424.	1.2	7
158	The diamond-solution interface: the surface energy of hydrogen terminated nanocrystalline CVD diamond derived from contact angle measurements. Materials Research Society Symposia Proceedings, 2011, 1362, 1.	0.1	0
159	Electrochemical sensor array for bioprocess monitoring. Electrochimica Acta, 2011, 56, 9673-9678.	5.2	20
160	Importance of Adjunctive Heart Failure Optimization Immediately After Implantation to Improve Long-Term Outcomes With Cardiac Resynchronization Therapy. American Journal of Cardiology, 2011, 108, 409-415.	1.6	55
161	Role of grain size in superconducting boron-doped nanocrystalline diamond thin films grown by CVD. Physical Review B, 2011, 84, .	3.2	36
162	Influence of methane concentration on the electric transport properties in heavily boron-doped nanocrystalline CVD diamond films. Materials Research Society Symposia Proceedings, 2011, 1282, 87.	0.1	1

#	Article	IF	CITATIONS
163	Tracing Gold Nanoparticle Charge by Electrolyteâ^'Insulatorâ^'Semiconductor Devices. Journal of Physical Chemistry C, 2011, 115, 4439-4445.	3.1	16
164	Eukaryotic cell lines as a sensitive layer for direct monitoring of carbon monoxide. Physica Status Solidi (A) Applications and Materials Science, 2011, 208, 1345-1350.	1.8	9
165	Towards a multiâ€sensor system for the evaluation of aseptic processes employing hydrogen peroxide vapour (H <sub>2</sub> O <sub>2</sub> ). Physica Status Solidi (A) Applications and Materials Science, 2011, 208, 1351-1356.	1.8	8
166	A siliconâ€based multiâ€sensor chip for monitoring of fermentation processes. Physica Status Solidi (A) Applications and Materials Science, 2011, 208, 1364-1369.	1.8	11
167	Miniaturised eightâ€channel impedance spectroscopy unit as sensor platform for biosensor applications. Physica Status Solidi (A) Applications and Materials Science, 2011, 208, 1357-1363.	1.8	22
168	Study on the giant positive magnetoresistance and Hall effect in ultrathin graphite flakes. Physica Status Solidi (A) Applications and Materials Science, 2011, 208, 1252-1258.	1.8	9
169	Monitoring of peptide induced disruption of artificial lipid membrane constructed on boronâ€doped nanocrystalline diamond by electrochemical impedance spectroscopy. Physica Status Solidi (A) Applications and Materials Science, 2011, 208, 2099-2103.	1.8	4
170	Realâ€ŧime study of protein adsorption on thin nanocrystalline diamond. Physica Status Solidi (A) Applications and Materials Science, 2011, 208, 2093-2098.	1.8	15
171	Engineering of Functional Interfaces. Physica Status Solidi (A) Applications and Materials Science, 2011, 208, 1216-1216.	1.8	0
172	Nanocrystalline diamond impedimetric aptasensor for the label-free detection of human IgE. Biosensors and Bioelectronics, 2011, 26, 2987-2993.	10.1	77
173	Impedimetric, diamond-based immmunosensor for the detection of C-reactive protein. Sensors and Actuators B: Chemical, 2011, 157, 130-138.	7.8	43
174	Separation of intra- and intergranular magnetotransport properties in nanocrystalline diamond films on the metallic side of the metal–insulator transition. New Journal of Physics, 2011, 13, 083008.	2.9	68
175	Optimization of a Boron Doped Nanocrystalline Diamond Temperature Regulator for Sensing Applications. Materials Research Society Symposia Proceedings, 2011, 1282, 123.	0.1	0
176	Rapid assessment of the stability of DNA duplexes by impedimetric real-time monitoring of chemically induced denaturation. Lab on A Chip, 2011, 11, 1656.	6.0	35
177	Metallization of Ultraâ€Thin, Nonâ€Thiol SAMs with Flat‣ying Molecular Units: Pd on 1, 4â€Dicyanobenzene. ChemPhysChem, 2010, 11, 2951-2956.	2.1	14
178	Real-time detection of CO by eukaryotic cells. Procedia Engineering, 2010, 5, 17-20.	1.2	5
179	In/extrinsic granularity in superconducting boron-doped diamond. Physica C: Superconductivity and Its Applications, 2010, 470, 853-856.	1.2	4
180	MIP-based sensor platforms for the detection of histamine in the nano- and micromolar range in aqueous media. Sensors and Actuators B: Chemical, 2010, 148, 392-398.	7.8	76

#	Article	IF	CITATIONS
181	Biological modification of carbon nanowalls with DNA strands and hybridization experiments with complementary and mismatched DNA. Chemical Physics Letters, 2010, 485, 196-201.	2.6	13
182	Customized impedance spectroscopy device as possible sensor platform for biosensor applications. Physica Status Solidi (A) Applications and Materials Science, 2010, 207, 919-923.	1.8	20
183	A MIPâ€based biomimetic sensor for the impedimetric detection of histamine in different pH environments. Physica Status Solidi (A) Applications and Materials Science, 2010, 207, 837-843.	1.8	50
184	Boron doped nanocrystalline diamond temperature regulator for sensing applications. Physica Status Solidi (A) Applications and Materials Science, 2010, 207, 2110-2113.	1.8	7
185	Diamond and Cubic Boron Nitride: Properties, Growth and Applications. AIP Conference Proceedings, 2010, , .	0.4	12
186	Granular superconductivity in metallic and insulating nanocrystalline boron-doped diamond thin films. Journal Physics D: Applied Physics, 2010, 43, 374019.	2.8	14
187	Magnetic field-driven superconductor–insulator transition in boron-doped nanocrystalline chemical vapor deposition diamond. Journal of Applied Physics, 2010, 108, .	2.5	9
188	Intrinsic granularity in nanocrystalline boron-doped diamond films measured by scanning tunneling microscopy. Physical Review B, 2009, 80, .	3.2	17
189	DNA Sensors with Diamond as a Promising Alternative Transducer Material. Sensors, 2009, 9, 5600-5636.	3.8	49
190	Negative magnetoresistance in boron-doped nanocrystalline diamond films. Journal of Applied Physics, 2009, 106, 033711.	2.5	11
191	Capacitive Field-effect (bio-)chemical Sensors Based on Nanocrystalline Diamond Films. Materials Research Society Symposia Proceedings, 2009, 1203, 1.	0.1	0
192	Diamond Nucleation by Carbon Transport from Buried Nanodiamond TiO <sub>2</sub> Sol el Composites. Advanced Materials, 2009, 21, 670-673.	21.0	32
193	Characterisation of capacitive field-effect sensors with a nanocrystalline-diamond film as transducer material for multi-parameter sensing. Biosensors and Bioelectronics, 2009, 24, 1298-1304.	10.1	24
194	Concept for a solid-state multi-parameter sensor system for cell-culture monitoring. Electrochimica Acta, 2009, 54, 6107-6112.	5.2	12
195	Nanocrystalline-diamond thin films with high pH and penicillin sensitivity prepared on a capacitive Si–SiO2 structure. Electrochimica Acta, 2009, 54, 5981-5985.	5.2	20
196	Synthetic diamond films as a platform material for labelâ€free protein sensors. Physica Status Solidi (A) Applications and Materials Science, 2009, 206, 520-526.	1.8	20
197	Diamondâ€based DNA sensors: surface functionalization and readâ€out strategies. Physica Status Solidi (A) Applications and Materials Science, 2009, 206, 391-408.	1.8	53
198	Preface: Phys. Status Solidi A 206/3. Physica Status Solidi (A) Applications and Materials Science, 2009, 206, 389-390.	1.8	0

#	Article	IF	CITATIONS
199	Chinese hamster ovary cell viability on hydrogen and oxygen terminated nano―and microcrystalline diamond surfaces. Physica Status Solidi (A) Applications and Materials Science, 2009, 206, 2042-2047.	1.8	13
200	AlN on nanocrystalline diamond piezoelectric cantilevers for sensors/actuators. Procedia Chemistry, 2009, 1, 40-43.	0.7	10
201	Diagnóstico y tratamiento de la anemia en pacientes con enfermedad renal crónica en todos sus estadios. Consenso del Anemia Working Group Latin America (AWGLA). Dialisis Y Trasplante, 2009, 30, 104-108.	0.4	1
202	A MIP-based impedimetric sensor for the detection of low-MW molecules. Biosensors and Bioelectronics, 2008, 23, 913-918.	10.1	93
203	Penicillin detection with nanocrystallineâ€diamond fieldâ€effect sensor. Physica Status Solidi (A) Applications and Materials Science, 2008, 205, 2141-2145.	1.8	25
204	Fourier-Transform Photocurrent Spectroscopy for a fast and highly sensitive spectral characterization of organic and hybrid solar cells. Thin Solid Films, 2008, 516, 7135-7138.	1.8	59
205	Topographical and Functional Characterization of the ssDNA Probe Layer Generated Through EDC-Mediated Covalent Attachment to Nanocrystalline Diamond Using Fluorescence Microscopy. Langmuir, 2008, 24, 9125-9134.	3.5	35
206	Structural and Optical Properties of DNA Layers Covalently Attached to Diamond Surfaces. Langmuir, 2008, 24, 7269-7277.	3.5	38
207	Nanocrystalline Diamond-Based Field-Effect Capacitive pH Sensor. , 2007, , .		0
208	Towards a Real-Time, Label-Free, Diamond-Based DNA Sensor. Langmuir, 2007, 23, 13193-13202.	3.5	66
209	pH sensitivity of nanocrystalline diamond films. Physica Status Solidi (A) Applications and Materials Science, 2007, 204, 2925-2930.	1.8	9
210	Observation of the subgap optical absorption in polymer-fullerene blend solar cells. Applied Physics Letters, 2006, 88, 052113.	3.3	158
211	EDC-mediated DNA attachment to nanocrystalline CVD diamond films. Biosensors and Bioelectronics, 2006, 22, 170-177.	10.1	63
212	High field magnetoresistivity of epitaxial La2â^'xSrxCuO4 thin films. Physica C: Superconductivity and Its Applications, 2005, 432, 81-98.	1.2	4
213	Impedimetric immunosensors based on the conjugated polymer PPV. Biosensors and Bioelectronics, 2005, 20, 2151-2156.	10.1	40
214	Absorption phenomena in organic thin films for solar cell applications investigated by photothermal deflection spectroscopy. Journal of Materials Science, 2005, 40, 1413-1418.	3.7	145
215	DNA attachment to nanocrystalline diamond films. Physica Status Solidi A, 2005, 202, 2212-2216.	1.7	29
216	Head-On Immobilization of DNA Fragments on CVD-Diamond Layers. Materials Science Forum, 2005, 492-493, 267-272.	0.3	6

#	Article	IF	CITATIONS
217	Low-level optical absorption phenomena in organic thin films for solar cell applications investigated by highly sensitive photocurrent and photothermal techniques. , 2004, , .		5
218	Influence of fluctuation conductivity on the high-field magnetoresistivity in epitaxial La2â^'xSrxCuO4 thin films. Physica B: Condensed Matter, 2004, 346-347, 339-343.	2.7	2
219	High field magnetotransport in high temparature superconductors. Physica C: Superconductivity and Its Applications, 2004, 404, 385-394.	1.2	4
220	Transport properties of La2â^'xSrxCuO4 epitaxial thin films in high magnetic fields. Physica C: Superconductivity and Its Applications, 2004, 404, 405-409.	1.2	0
221	Covalent immobilization of DNA on CVD diamond films. Physica Status Solidi A, 2003, 199, 44-48.	1.7	23
222	Sign inversion of the high-field Hall slope in epitaxialLa0.5Ca0.5MnO3thin films. Physical Review B, 2003, 68, .	3.2	11
223	In-plane paraconductivity inLa2â°'xSrxCuO4thin film superconductors at high reduced temperatures:â€,Independence of the normal-state pseudogap. Physical Review B, 2003, 68, .	3.2	36
224	Orbital Ordering and the Cooperative Jahn–Teller Effect in Single Crystals of the Magnetic Perovskite La7/8Sr1/8MnO3. Advances in Quantum Chemistry, 2003, 44, 563-578.	0.8	0
225	Universal behavior of the in-plane paraconductivity of cuprate superconductors in the short-wavelength fluctuation regime. Physical Review B, 2002, 65, .	3.2	18
226	EVIDENCE FOR THE PAIR FORMATION FAR ABOVE Tc IN EPITAXIAL La2-xSrxCuO4 THIN FILMS. International Journal of Modern Physics B, 2002, 16, 3223-3226.	2.0	0
227	Colossal Negative Magnetoresistivity of Nd0.5Sr0.5MnO3 Films in Fields up to 50 T. , 2002, , 481-486.		0
228	Spin-dependent hopping in the paramagnetic state of the bilayer manganite (La 0.4 Pr 0.6 ) 1.2 Sr 1.8 Mn 2 O 7. Europhysics Letters, 2002, 58, 285-291.	2.0	17
229	High field transport properties of La Sr CuO epitaxial thin films. European Physical Journal B, 2002, 29, 369-375.	1.5	5
230	Transition to the normal state of superconducting Y1Ba2Cu3O7-Άthin films induced by high current densities. Superconductor Science and Technology, 2001, 14, 748-753.	3.5	9
231	Hâ^'Tmagnetic phase diagrams of electron-dopedSm1â^'xCaxMnO3:  Evidence for phase separation and metamagnetic transitions. Physical Review B, 2001, 63, .	3.2	75
232	Temperature dependent memory effects in the bilayer manganite(La0.4Pr0.6)1.2Sr1.8Mn2O7. Physical Review B, 2001, 64, .	3.2	37
233	Influence of the morphology on the magneto-transport properties of laser-ablated ultrathin La0.7Ba0.3MnO3 films. Journal of Applied Physics, 2001, 90, 1429-1435.	2.5	2
234	Transport properties at the insulator–superconductor phase boundary of La2â^'xSrxCuO4 thin films. Physica C: Superconductivity and Its Applications, 2001, 356, 107-114.	1.2	9

#	Article	IF	CITATIONS
235	Scaling of the transport properties in theY1â^'yPryBa2Cu3Oxsystem. Physical Review B, 2001, 64, .	3.2	21
236	Comparison of the transport mechanism in underdoped high-temperature superconductors and in spin ladders. Physica C: Superconductivity and Its Applications, 2000, 337, 260-264.	1.2	1
237	Normal state resistivity of underdoped YBa2Cu3O7-d films and La2-XSrXCuO4 ultra-thin films in fields up to 60 T. Physica C: Superconductivity and Its Applications, 2000, 341-348, 903-904.	1.2	1
238	Stripe formation and disorder induced stripe fragmentation. Physica C: Superconductivity and Its Applications, 2000, 341-348, 1799-1802.	1.2	0
239	INTERPLAY BETWEEN TRANSPORT, MAGNETIC-, AND STRUCTURAL PROPERTIES OF MN-PEROVSKITES WITH VARIOUS DOPING LEVEL. International Journal of Modern Physics B, 2000, 14, 3735-3740.	2.0	2
240	Influence of the cooperative Jahn-Teller effect on the transport and magnetic properties ofLa7/8Sr1/8MnO3single crystals. Physical Review B, 2000, 61, 529-537.	3.2	23
241	Comparative Hall studies in the electron- and hole-doped manganitesLa0.33Ca0.67MnO3andLa0.70Ca0.30MnO3. Physical Review B, 2000, 62, 11633-11638.	3.2	22
242	Wagneret al.Reply:. Physical Review Letters, 2000, 84, 4018-4018.	7.8	5
243	HIGH-FIELD MAGNETOTRANSPORT OF EPITAXIAL LA2-XSRXCUO4 THIN FILMS IN THE REGIME OF LOW SR-DOPING. International Journal of Modern Physics B, 2000, 14, 3747-3752.	2.0	1
244	Title is missing!. Journal of Low Temperature Physics, 1999, 117, 681-685.	1.4	13
245	Spin Dependent Hopping and Colossal Negative Magnetoresistance in EpitaxialNd0.52Sr0.48MnO3Films in Fields up to 50 T. Physical Review Letters, 1998, 81, 3980-3983.	7.8	148
246	Carrier density variation in films of Nd 0.5 Sr 0.5 MnO 3. Europhysics Letters, 1998, 41, 49-54.	2.0	38
247	Anomalous Hall effect in thin films ofPr0.5Sr0.5MnO3. Physical Review B, 1997, 55, R14721-R14724.	3.2	24
248	Magnetotransport in epitaxial thin films of the magnetic perovskitePr0.5Sr0.5MnO3. Physical Review B, 1997, 55, 3699-3707.	3.2	40
249	Hopping conductivity of magnetic polarons in epitaxial Pr0.5Sr0.5MnO3 films. European Physical Journal D, 1996, 46, 2005-2006.	0.4	Ο
250	Dimensional crossover in the pinning of heavy-ion irradiated Bi-2212 films. Physica C: Superconductivity and Its Applications, 1996, 259, 142-150.	1.2	7
251	Fermi surfaces of Bi2Sr2CaCu2O8+l ´ thin film. Physica C: Superconductivity and Its Applications, 1996, 261, 153-156.	1.2	2
252	Matching and surface barrier effects of the flux-line lattice in superconducting films and multilayers. Physical Review B, 1996, 53, 8658-8670.	3.2	34

#	Article	IF	CITATIONS
253	Magnetic Transitions and Magneto-Transport in Epitaxial Pr <sub>0.5</sub> Sr <sub>0.5</sub> MnO <sub>3</sub> Thin Films. European Physical Journal Special Topics, 1996, 06, C3-309-C3-314.	0.2	0
254	Thermally assisted flux flow in epitaxial Bi2Sr2Ca2Cu3O10+? thin films: Estimation of the anisotropy parameter. Journal of Superconductivity and Novel Magnetism, 1995, 8, 293-297.	0.5	4
255	Vortex unbinding and layer decoupling in epitaxialBi2Sr2Ca2Cu3O10+δfilms. Physical Review B, 1995, 52, 4553-4558.	3.2	37
256	Bose-glass behavior of the vortex system in epitaxialBi2Sr2CaCu2O8+Î films with columnar defects. Physical Review B, 1995, 51, 3953-3956.	3.2	30
257	Evidence for a vortex-liquid–vortex-glass transition in epitaxialBi2Sr2Ca2Cu3O10+δthin films. Physical Review B, 1995, 51, 1206-1212.	3.2	53
258	Phase-slip dissipation and dimensionality above the irreversibility line inBi2Sr2CaCu2O8+x. Physical Review B, 1994, 50, 12920-12926.	3.2	15
259	Nernst, Seebeck, and Hall effects in the mixed state ofYBa2Cu3O7â~δandBi2Sr2CaCu2O8+xthin films: A comparative study. Physical Review B, 1994, 50, 3312-3329.	3.2	146
260	Characterization of YBa2Cu3O7/PrBa2Cu3O7 superlattices. Journal of Superconductivity and Novel Magnetism, 1994, 7, 197-200.	0.5	4
261	Characterization of epitaxial Bi2Sr2CaCu2O8+? thin films. Journal of Superconductivity and Novel Magnetism, 1994, 7, 217-219.	0.5	4
262	In situ-preparation, characterization and transport-properties of high quality Bi2Sr2CaCu2Oy-thin films. Physica B: Condensed Matter, 1994, 194-196, 2193-2194.	2.7	0
263	Thermally activated dissipation in epitaxial Bi2Sr2CaCu2O8 + δ films evidence for the occurence of vortex strings with three-dimensional fluctuations in low magnetic fields. Physica C: Superconductivity and Its Applications, 1994, 234, 249-254.	1.2	15
264	Heavy-ion-induced effects on the transport critical current density in epitaxial 2212-BSCCO thin films. Physica C: Superconductivity and Its Applications, 1994, 235-240, 2971-2972.	1.2	7
265	Scaling behavior of U(I)-characteristics and zero-field resistive transitions in epitaxial Bi2Sr2CaCu2O8+l̃´thin films. Physica C: Superconductivity and Its Applications, 1994, 235-240, 3165-3166.	1.2	1
266	Comparative study of the magnetoresistivity of YBa2Cu3O7â^δand Bi2Sr2Ca Cu2O8+x epitaxial thin films in the fluktuation regime. Physica C: Superconductivity and Its Applications, 1994, 235-240, 1933-1934.	1.2	1
267	A systematic comparison of transport properties and pinning potentials in YBCO and BiSCCO thin films. Physica C: Superconductivity and Its Applications, 1994, 235-240, 2625-2626.	1.2	3
268	Pinning and irreversibility behavior in Au-irradiated Bi-2212 films. Physica C: Superconductivity and Its Applications, 1994, 235-240, 2739-2740.	1.2	2
269	Thermally activated flux movement and critical transport current density in epitaxialBi2Sr2CaCu2O8+δfilms. Physical Review B, 1994, 49, 13184-13192.	3.2	54

270 Vortex State and Dimensionality. , 1994, , 293-302.

#	Article	IF	CITATIONS
271	High-Tc-based Josephson-junctions and SQUIDs by mechanically induced growth disorder. European Physical Journal Special Topics, 1994, 04, C6-217-C6-222.	0.2	0
272	AC conductivity in superconducting YBa2Cu3O7 and Bi2Sr2CaCu2O8 thin films. Physica B: Condensed Matter, 1993, 186-188, 986-988.	2.7	1
273	Preparation and structural characterization of thin epitaxial Bi2Sr2CaCu2O8+l̂´films with Tc in the 90 K range. Physica C: Superconductivity and Its Applications, 1993, 215, 123-131.	1.2	54
274	PINNING FORCE DENSITY IN YBa2Cu3O7-FILMS AND YBa2Cu3O7/PrBa2Cu3O7-SUPERLATTICES. International Journal of Modern Physics B, 1993, 07, 135-138.	2.0	0
275	ANISOTROPIC SUPERCONDUCTING PROPERTIES OF YBa2Cu3O7 BASED THIN FILMS AND SUPERLATTICES. International Journal of Modern Physics B, 1993, 07, 113-122.	2.0	0
276	Enhancement of critical current density by confinement of vortices in Bi2Sr2CaCu2Oxsingle crystals and thin films. Applied Physics Letters, 1993, 63, 2821-2823.	3.3	12
277	Scaling of the angular dependence of the critical current density in high-Tcsuperconductors. Physical Review B, 1993, 47, 12099-12103.	3.2	29
278	Impurity pinning in epitaxial YBa/sub 2/(Cu/sub 1-x/TM/sub x/)/sub 3/O/sub 7- delta / (TM=Zn, Ni)-thin films. IEEE Transactions on Applied Superconductivity, 1993, 3, 1468-1471.	1.7	3
279	Superconducting transport properties of Bi2Sr2CaCu2O8+xbicrystal grain boundary junctions. Applied Physics Letters, 1993, 63, 996-998.	3.3	47
280	COMPLEX CONDUCTIVITY IN THIN FILMS OF YBa2Cu3O7 AND YBa2(Cu1â^'xMx)3O7 WITH M = Zn AND Ni. International Journal of Modern Physics B, 1993, 07, 139-142.	2.0	0
281	Contribution of Zn Impurity Atoms to the Anisotropic Pinning Force Density of Thin Epitaxial YBa <sub>2</sub> (Cu <sub> 1- <i>x</i> </sub> Zn <sub> <i>x</i> </sub> ) <sub>3</sub> O <sub>7-î</sub> Films. Europhysics Letters, 1992, 18, 641-646.	2.0	7
282	Superconductivity and transport properties of epitaxial YBa2(Cu1-xZnx)3O7-thin films. Superconductor Science and Technology, 1992, 5, S133-S136.	3.5	2
283	In situ-preparation of Bi2Sr2CaCu2Oy-thin films by DC-sputtering. Physica C: Superconductivity and Its Applications, 1992, 195, 258-262.	1.2	40
284	Thermally activated flux-flow in epitaxially grown YBa2(Cu1â^'χZnχ)3O7â^' thin films. Physica C: Superconductivity and Its Applications, 1991, 185-189, 2175-2176.	1.2	6
285	Growth of high quality YBa2Cu3O7 films on various substrate materials and influence of Zn-doping on superconductivity. Physica C: Superconductivity and Its Applications, 1990, 171, 231-237.	1.2	41